An Improved Iris Recognition Method Based on Discrete Cosine Transform and Gabor Wavelet Transform Algorithm

Xiao-hong Chen, Jie-sheng Wang*, Yan-lang Ruan, Shu-zhi Gao

Abstract—**An improved Iris recognition method was proposed by adopting the discrete cosine transform (DCT) method and Gabor wavelet transform algorithm. The combination of the calculus operator method, improved Hough transform and the two-step edge detection method is adopted to realize the iris localization and extraction. The discrete cosine transform method and the Gabor wavelet transform are utilized to form the propose improved Gabor wavelet transform for iris localization and extraction. Finally, the nearest neighbor distance detector and Euclidean distance are used as the classifier to realize the iris recognition. Simulation experiments are carried out to prove the effectiveness of the proposed strategy.**

Index Terms—**Iris recognition, Gabor wavelet transform algorithm, discrete cosine transform method**

I. Introduction

THE appearance of the eye is composed of scleroses, iris and pupil. The scleroses are the peripheral white part of the eyeball, accounting for 30% of the area of the eye. The central part of the eye is the pupil, which accounts for about 5%. The iris contains the rich texture information, which is about 65%. By the age of 12, the iris has basically developed enough to enter a relatively stable period. The iris can be used as a material basis for identification because of its high uniqueness, stability and unalterable characteristics.

In general, the eye images must be tackled so as to reduce noises, enhance the images and extract the iris. In 1984, a super-resolution method in the frequency domain was firstly proposed to enhance the images [1-2]. The difference methods are adopted to expand the image sampling points [3-7]. The repeat back projection method is to carry out the repeated application of low resolution images and estimation of the difference of high-resolution images to update the estimated high resolution images [8-9]. The convex projection method is one of the important algorithms to solve the super-resolution image restoration problem [10-11]. The partial differential equation algorithm is used to tackle with the change of images by utilizing the partial differential equations under some mechanism and find the proper form to reflect its proper image change. The horizontal line method is the unified coding of the connected gray area in the image. After years of hard work, Froment and Whitaker have solved some problems in the application of the horizontal line method. In the Iris recognition algorithm, the iris normalization, feature extraction and classifier are important components [12-15]. Currently, the internationally influential algorithms include Daugman's phase encoding method [16-18], Wilde's Laplacian pyramid based image matching method [19-20], Bole's one-dimensional wavelet zero-crossing detection method [21], Tan Tieniu's two-dimensional texture analysis method based on Gabor filter [22-23], Lim's method based on Haar wavelet analysis [24-25], etc. All of these methods are based on grayscale images in that the grayscale images have provided enough identification information, and the color of the iris is not an important information.

This paper proposed an improved Iris recognition method based on discrete cosine transform and Gabor wavelet transform algorithm. Firstly, the image of the human eye was tackled to locate the inner and outer circle of the iris, extract the iris part, and then filter the extracted iris. Then, the modified Gabor wavelet transform was adopted to extract features and realize feature reduction of iris images. Finally, the iris images were classified by the closest classifier and Euclidean distance, and the test images were successfully identified.

II. Iris Positioning and Extraction

In general, in the process of collecting iris images, the image of the iris part cannot be directly obtained in that the collected image contains all the human eyes information. For iris recognition, the collected eye image must be divided to retain the image with the iris part so that it can increase the recognition accuracy. The essence of iris segmentation is to divide the iris region that is needed for later recognition from the captured image of the human eye, which is also called iris localization. The iris structure distribution of the human eye presents certain geometric features, and the inner and outer boundary of the iris are approximately two circles. Therefore, this geometric feature of iris can be used to divide them.

Manuscript received November 21, 2018; revised January 26, 2019. This work was supported by the the Basic Scientific Research Project of Institution of Higher Learning of Liaoning Province (Grant No. 2017FWDF10), and the Project by Liaoning Provincial Natural Science Foundation of China (Grant No. 20180550700).

Xiao-Hong Chen is with the School of Mechanical Engineering and Automation, University of Science and Technology Liaoning, Anshan, 114051, PR China. (e-mail: l: ascxh@163.com).

Jie-Sheng Wang is with the School of Electronic and Information Engineering, University of Science and Technology Liaoning, Anshan, 114051, PR China; National Financial Security and System Equipment Engineering Research Center, University of Science and Technology Liaoning. (Corresponding author, phone: 86-0412-2538355; fax: 86-0412-2538244; e-mail: wang_jiesheng@126.com).

Yan-lang Ruan is with the School of Electronic and Information Engineering, University of Science and Technology Liaoning, Anshan, 114051, PR China (e-mail:ruanyanlang@163.com).

Shu-Zhi Gao is with Shenyang University of Chemical Technology, Shenyang, 110000, PR China (e-mail: szg6868@126.com).

However, because the pupils are affected by factors, such as the external light, the size of the pupils will show a different degree of contraction with these external influences. So the inner and outer boundaries of the iris are actually two approximate circles with different centers.

A. Iris Localization and Extraction Based on Calculus Operator

Dr. Daugman proposed an iris localization method to locate the iris [26], which adopts the circular detector to detect the boundary circle of the iris, and the circular detector is calculated by the differential integral. The curve integral calculation is realized by Eq. (1).

$$\max_{(r,y_0,x_0)}\left|G_\sigma(r)\cdot\frac{\partial}{\partial r}\int_{(y_0,x_0)}\frac{I(x,y)}{2\pi r}ds\right| \tag{1}$$

where, (y_0,x_0) represents all points that can form a point coordinate of the center of the circle, r is a variable and it is constantly changing, and $I(y,x)$ represents the grayscale value of the pixel point (y,x).

The concrete operation process of the calculus operator on the image is described as follows. By gradually increasing the radius r, the arc d with the center of a circle (y_0,x_0) and radius r are carried out the integral calculation. After obtaining the line integral, $I(y,x)$ is averaged and the calculated s is carried out the partial derivatives operation until the directional derivative reaches the maximum value along the gradient direction, that is to say the the calculated gradient direction is the direction that the function $I(x,y)$ increases with the fastest velocity. For a circle, this direction is the direction of its radius. Thus a circle is determined with a fixed center and radius. The function of $G_\sigma(r)$ is a smoothing filter to reduce noises and facilitate the boundary detection, whose concrete expression is shown in Eq. (2).

$$G_\sigma(r)=\frac{1}{\sqrt{2\pi}\sigma}e^{-\frac{(r-r_0)^2}{2\sigma^2}} \tag{2}$$

Then this circle is carried out the convolve operation with the Gaussian function $G_\sigma(r)$, which is effective to realize the edge gradient filter and obtains the approximate circle round the edge of iris both inside and outside. It is the biggest round among the adjacent rounds with the maximum average gray level gradient. In order to improve efficiency, Eq. (1) needs to be discretized, whose discretization algorithm is shown in Eq. (3).

$$\max_{(n\Delta r,x_0,y_0)}\left|\frac{1}{\Delta r}\sum_k\left\{\left(G_\sigma(n-k)\Delta r-G_\sigma\left((n-k-1)\Delta r\right)\sum_m I\left(x',y'\right)\right)\right\}\right| \tag{3}$$

where, $x'=k\Delta r\cos(m\Delta\theta)+x_0$, $y'=k\Delta r\sin(m\Delta\theta)+y_0$.

Through the above calculation process, the iris edge location is the calculation of the maximum circular gray-scale changes in fact. It should be payed attention to the problem that the gray gradient between the sclera and the pupil is very small. In order to prevent the denominator from zero, a small gray scale must be added to the denominator of the function, so that the iris image is accurately positioned. The adopted discrete function is shown in Eq. (4).

$$\max\left(n\Delta r,x_0,y_0\right)\left|\sum_k\frac{\left(G_\sigma\left((n-k)\Delta r\right)-G_\sigma\left((n-k-1)\Delta r\right)\right)I\left(x',y'\right)}{\Delta r\sum_m I\left[\left((k-2)\Delta r\cos\left(m\Delta\theta\right)+x_0\right),\left((k-2)\Delta r\sin\left(m\Delta\theta\right)+y_0\right)\right]}\right| \tag{4}$$

The calculus operator to realize Iris localization has high accuracy and robustness. However, when locating the center of the circle and the radius, the center and the corresponding radius must be repeated, which greatly increases the amount of calculation. After locating the inner and outer circle of the iris, the iris is extracted.

All the pixel points are checked in sequence, and their distances to the center of the circle and the radius of the circle are compared. Then by dividing points inside and outside, the pixels within the circle part and outside the cylindrical part are directly set to 255, and the unnecessary parts are removed and keep the needed iris parts. In this way, the localized iris part is extracted. The images in the Casia's eye database are used to conduct the simulation experiments. The results of iris localization experiments are shown in Fig. 1 and Fig. 2. The center coordinate of the inner circle is (168,152) and the radius r is 36. The center of the outer circle is (170,157) and the radius R is 106. It can be seen from Fig. 2 that the calculus operator locating the iris achieves a better positioning effect.

Fig. 1 Iris location results based on the calculus operator.

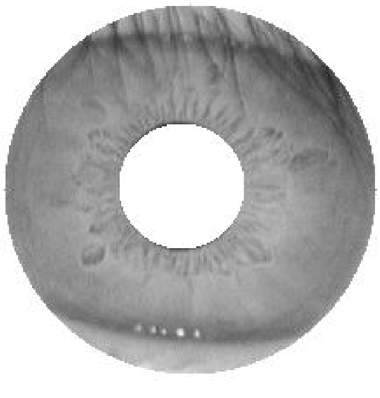

Fig. 2 Obtained iris.

B. Hough Transform and Edge Detection

The principle of Hough transform is to map the image space to the parameter space. The basic idea is the duality of points and lines, which is used to map the points on the same line in the image space to the intersection line in the parameter space. A two-step positioning method was proposed by using edge detection and Hough transformation to locate the iris. Firstly, the human eye image is binarized, and the edge points are detected and parameterized.

Then the circle parameters that can form the edge of the circle are voted in the circle. The circle parameter with the highest number of votes is the inner and the outer boundary of the iris that need to be located. It is necessary to filter the human eye images to eliminate the effects of eyelids and eyebrows on the binarization. The median filter processing results are shown in Fig. 3. The gradient-based edge detection operator is expressed as follows.

$$\left|\nabla G(x,y)*I(x,y)\right|, G(x,y)=\frac{1}{2\pi\sigma^2}e^{-\frac{(x-x_0)^2+(y-y_0)^2}{2\sigma^2}} \tag{5}$$

where, $\nabla \equiv (\partial/\partial x, \partial/\partial y)$ represents the two-dimensional Laplace operator, $*$ represents the convolution operation, $G(x,y)$ is a two-dimensional Gaussian function, whose role is to eliminate noises in order to facilitate the detection of gradient changes at the boundary, and $I(x,y)$ represents the gray value of the image at (x,y). The two-dimensional Gaussian function and Laplacian differential operator are combined to proceed the image convolution so as to obtain a set of two groups of points. The set of points in these two groups includes the iris inner edge points and the outer edge points. For obtaining the iris inner circle boundary points, the traditional method is modified to determine the center of the inner circle firstly. The obtained center coordinates are shown in Fig. 4.

Fig. 3 Median filtering.

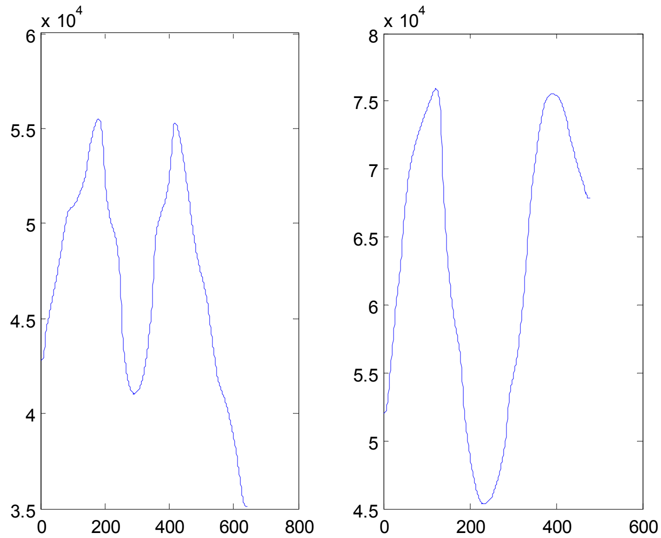

Fig. 4 The center of the iris.

When the center of inner circle is fixed, this center is as the parent point for area growth. It stops growing when the area grows to the inner circle edge, and this area is extracted after the growth of the border. This belongs to the wanted border of the iris inner circle. On the other hand, the edge detection of iris outer circle is carried out according to the traditional method. The results on the Iris edge detection tests are shown in Fig. 5 and Fig. 6. The Hough transform algorithm can be defined in Eq. (6)-(8).

$$H(x_0,y_0,r)=\sum_{i=1}^{n}h(x_i,y_i,x_0,y_0,r) \tag{6}$$

$$h(x_i,y_i,x_0,y_0,r)=\begin{cases}1, g(x_i,y_i,x_0,y_0,r)=0\\ 0, Other\end{cases} \tag{7}$$

$$g(x_i,y_i,x_0,y_0,r)=(x_i-x_0)^2-(y_i-y_0)^2-r^2 \tag{8}$$

When H appears its maximum, it can be determined that the boundary points pass through the circle, that is to say this circle can be regarded as the outline circle of boundary. Each circle has a definite center (x,y) and a radius r. The three quantities (x , y , r) form a set of circle parameters. The complexity of the Hough transform is proportional to the number of parameters. The amount of calculation in theory is is exponentially growth with the number of these parameters. The Hough transform without interruption of the curves can effectively reduce the noise interference. However, the calculation of Hough transform is large and time-consuming, and it also takes up memory. After locating the inner and outer circle of the iris, the iris can be extracted. Its principle is consistent with the calculus iris extraction method, which directly compares the distance of all the pixels to the center with the size of the radius and divides the inside and outside points based on the compared results.

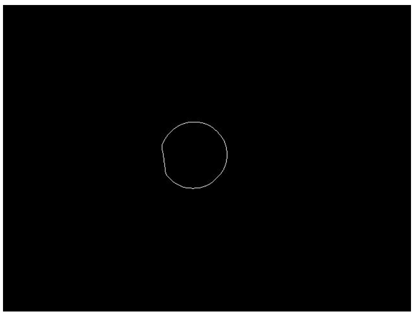

Fig. 5 The inner circle of iris.

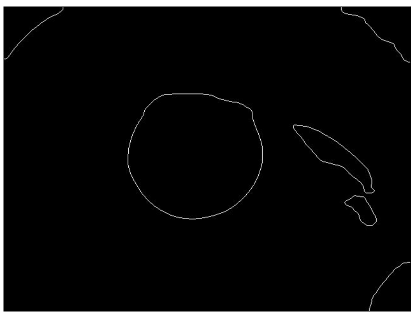

Fig. 6 The outer circle of iris.

The pixels inside the inner circle and the outer circle are set as 255 directly, making them white, that is to remove the unnecessary parts and keep the needed iris part. Thus the localized iris part is extracted. The images from Casia's eye database are adopted to conduct the simulation experiment and the results based on the two-steps iris localization method are shown in Fig. 7 and Fig. 8. The located inner circle center coordinate is (236,300) and the radius r is 52. The outer circle center coordinates is (234,299) and the radius R is 105. It can be seen from Fig. 7 and Fig. 8 that the adopted two-steps method can also be used to locate the iris.

III. Iris Normalization Unfolds

After extracting the iris area, because the pupil itself may have the shrinking and enlargement cases, and the collected human eye images may have translation, rotation and scaling problems. In order to reduce the impact of these factors, it is necessary to normalize the collected iris images. Iris normalization process maps the iris ring region into a rectangular region by the coordinate transformation. The length of the rectangular area is the angular resolution and the width is the radial resolution. After normalization, these external disturbances can be effectively reduced. The mapping operator can be described as:

$$I\left(x(r,\theta),y(r,\theta)\right)\rightarrow I(r,\theta) \tag{9}$$

$$\begin{cases} x(r,\theta)=(1-r)x_i(\theta)+rx_0(\theta) \\ y(r,\theta)=(1-r)y_i(\theta)+ry_0(\theta) \end{cases} \tag{10}$$

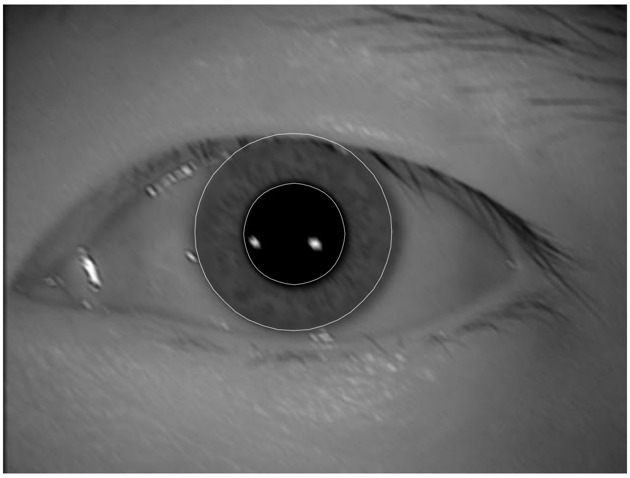

Fig. 7 Two step method for iris location.

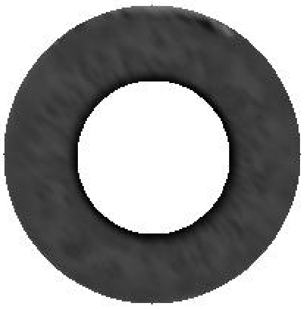

Fig. 8 Obtained iris.

After using the above mapping strategy, the iris is in polar coordinates. Because the extracted iris is circular, the iris image presents a rectangle in polar coordinates (r,θ). The Iris normalization method is described as follows. Seen from the data of the inner and outer circle centered by the iris, the center of inner circle and outer circle is not a point, where there is a certain deviation. The iris schematic diagram is shown in Fig. 9.

$O_2P=R$ represents the radius of the outer circle, $O_1P=r$ represents the radius of the inner circle, the center of the outer circle is (x_2,y_2), and the center of the inner circle is (x_1,y_1). The distance between the inner circle and the outer circle is calculated by Eq. (11).

$$\Delta r=\sqrt{(x_1-x_2)^2+(y_1-y_2)^2} \tag{11}$$

The angle between the horizontal line with the center of inside and outside circle is calculated by Eq. (12).

$$\phi=\arctan\frac{y_2-y_1}{x_2-x_1} \tag{12}$$

The Eq. (13) is used to calculate the outer radius R.

$$(r\cos\theta+\Delta r\cos\phi)^2+(r\cos\theta+\Delta r\sin\phi)^2=R^2 \tag{13}$$

Eq. (11) can be expanded as:

$$r^2+2\Delta r(\cos\theta\cos\phi+\sin\theta\sin\phi)r+\Delta r^2-R^2=0 \tag{14}$$

The inner circle radius r is calculated by Eq. (15).

$$r=-\Delta r\cos(\theta-\phi)+\sqrt{R^2-(\Delta r\sin(\theta-\phi))^2} \tag{15}$$

When the center and the corresponding radius of the inner and outer circle of the iris have been obtained, the quantities in the above equations are known. The iris area can be normalized by expanding the inner and outer edges of the pupil. The iris normalization is realized by Eq. (16)-(19).

$$r(\theta)=-\Delta r\cos(\theta-\phi)+\sqrt{R^2-(\Delta r\sin(\theta-\phi))^2} \tag{16}$$

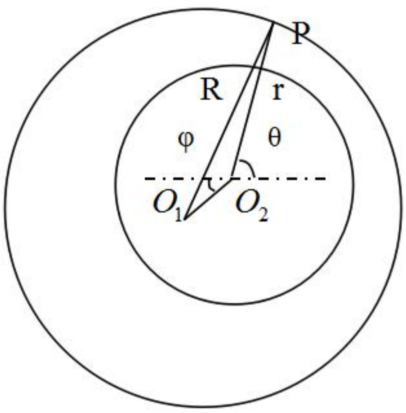

Fig. 9 Iris sketch.

$$x = x_2 + r(\theta)\cos(\theta) \quad (17)$$

$$y = y_2 - r(\theta)\sin(\theta) \quad (18)$$

$$Normalrize(i, j) = I(x, y) \quad (19)$$

where, $i = 1,2,3,\ldots M$, $j = 1,2,3,\ldots N$, and $\theta = j \times \theta/180$.

In the angle direction, the resolution must take the perimeter of the inner boundary, which is N pixel points with the smallest perimeter so that all the angles can reach this resolution. In the radial direction, the resolution M should select the radius of the inner and outer circle of the iris as the radius resolution so that the radial direction can be resolved in any direction. In this case, when using the extraction of Iris based on the calculus operator method, M is 58 and N is 496. When using Hough transform and edge detection to extract iris normalization again, M is 83 and N is 719. After normalization, the experimental results of Histogram equalization are shown in Fig. (10)-(13).

IV. Iris Recognition by Improved Gabor Wavelet

A. *Classical Algorithms of Iris Feature Extraction*

1. Daugman's Iris Texture Feature Extraction Algorithm

This method is a phase analysis method, whose principle is to use the calculus operator to locate the iris first, and then uses the Gabor wavelet transform to extract texture features. The coding method of iris recognition is shown in Fig. (14). It must be pointed out that this method does not adopt the amplitude information of filter results as iris characteristics, and uses the phase quantization method to code the phase information of the iris textures so that the characteristic code of the binary is constructed. That is to say that the character coding of the real part and the imaginary part of the filtering result are set up.

Fig. 10 Calculus operator method for Iris location, normalization and expansion.

Fig. 11 Histogram equalization.

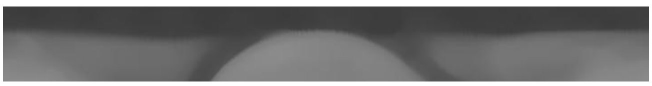

Fig. 12 Result of Iris localization, normalization and expansion.

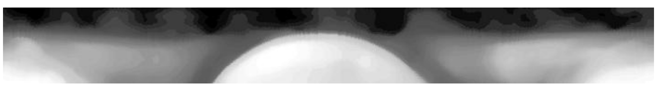

Fig. 13 Histogram equalization.

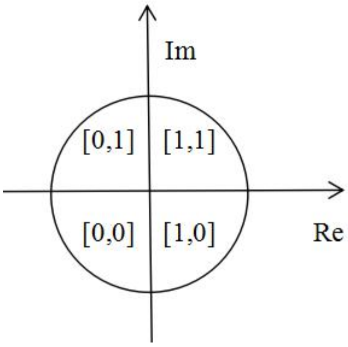

Fig. 14 Coding method of Iris recognition.

The specific coding method is described as follows. Each plural result is recorded using two binary numbers. If the real part is greater than or equal to 0, the first characteristic is set as 1, otherwise 0. Similarly, if the imaginary part is greater than or equal to 0, then the second eigenvalue is 1, otherwise 0. Finally, the Hamming distance classifier is adopted for classification decision.

2. Wildes Iris Texture Feature Extraction Algorithm

Prof. Wildes presented an image matching algorithm based on the Laplace pyramid (multi-scale matching recognition algorithm), whose principle is to filter the Iris images by using a Gaussian filter template and construct a 4-layer Laplace pyramids to extract the Iris texture. The Laplace-Gauss filter is defined as:

$$-\frac{1}{\pi\sigma^4}\left(1-\frac{\rho^2}{2\sigma^2}\right)e^{-\frac{\rho^2}{2\sigma^2}} \quad (20)$$

where, σ represents the standard deviation of the Gaussian function, and ρ represents the radial distance from the point in the image to the center of the filter.

The Laplacian of Gaussian (LOG) is used to decompose the iris images on the isotropic frequency bands so as to form the Laplace pyramid. $W = w^T w$ is adopted to form a low-pass filter, where $w = (1/16)[1,4,6,4,1]$. Given a picture I , W and I are carried out the convolved operation to obtain the filtered image g_k , whose function can be expressed as:

$$g_k = (W * g_{k-1})_{\downarrow 2} \quad (21)$$

where, $g_0 = I$, and $()_{\downarrow 2}$ represents a reduced sampling with coefficient 2 at the latitude of each image. The relationship between I_k , g_k and g_{k+1} can be expressed as:

$$I_k = g_k - 4W * (g_{k+1})_{\uparrow 2} \quad (22)$$

where, $()_{\uparrow 2}$ represents an expanded sampling with coefficient 2 in the rows and columns of the original image.

After four iterations, a 4-stage Laplace pyramids are set up. Then the picture p_1 and p_2 are converted into the sequence $p_1[i, j]$ and $p_2[i, j]$ of $m \times n$, and the standardized p_1 and p_2 can be expressed as:

$$corr\left(p_1,p_2\right)=\frac{\sum_{i=1}^{n}\sum_{j=1}^{m}\left(p_1[i,j]-\mu_1\right)\left(p_2[i,j]-\mu_2\right)}{nm\sigma_1\sigma_2} \tag{23}$$

where, μ_1 and μ_2 represent the average of p_1 and p_2, $\mu_k=(\sum_{i=1}^{n}\sum_{j=1}^{m}p_k[i,j])/(nm)$, $k=1,2$； σ_1 and σ_2 are the standard deviations of p_1 and p_2 , $\sigma_k=\sqrt{(\sum_{i=1}^{n}\sum_{j=1}^{m}\left(p_k[i,j]-\mu_k\right)^2)/(nm)}$, $k=1,2$.

Because this method takes advantage of all the possible Iris texture information, it relatively needs a large amount of calculation, which is its biggest drawback. But this characteristic makes the method be able to obtain the better distinguished different iris images.

3. Bole Iris Feature Extraction Method

Boles proposed an iris recognition algorithm, which is a zero-crossing detection algorithm. Since this method adopts the wavelet transform zero crossing technique, it has established a one-dimensional expression of the grey degree contour of iris. The method is centered on the center of the iris, and the iris images are sampled at intervals. The two-dimensional iris image is transformed into a one-dimensional signal $f\left(x\right)$, and the wavelet function is the second derivative of the smooth function $\theta\left(x\right)$.

$$\psi\left(x\right)=\frac{d^2}{dx^2}\theta\left(x\right) \tag{24}$$

where, $\theta\left(x\right)$ is the Gauss smoothing function.

The second derivative of the Gauss function and the signal function $f\left(x\right)$ are carried out the wavelet transform, which can be expressed as:

$$W_sf\left(x\right)=\psi_s\left(x\right)*f\left(x\right)=s^2\frac{d^2}{dx^2}\left(f\left(x\right)*\theta\left(x\right)_s\right) \tag{25}$$

where, $\theta_s\left(x\right)=(1/s)\theta\left(x/s\right)$, $s\in R$ and $s\neq 0$, which is named as the scale factor.

It can be seen from the above equation that the wavelet transform result of $f\left(x\right)$ is directly proportional to the second derivative of $f\left(x\right)$ after the smooth filtering operation. Then the zero crossing point Z_n of $W_sf\left(x\right)$ is recorded. Mallat proposed that it is only necessary to record the position Z_n of each zero cross point in $W_sf\left(x\right)$ and the integral value of the transformation result between any two adjacent zero crossings.

$$e_n=\int_{Z_{n-1}}^{Z_n}W_sf\left(x\right)dx \tag{26}$$

Through the above principle, some iterative computing can be used to reconstruct the signal $f(x)$. The extracted iris image is $f\left(x\right)$, so the obtained $[Z_{n.}e_n]_{n\in Z}$ can be named as the eigenvalue of the iris. The advantage of this method is that the iris image drift, rotation and proportion invariant are not sensitive to the brightness change and noises.

B. Gabor Wavelet Transform

The Gabor wavelet transform is a wavelet transform based on the Gabor function, which can be used to analyze all kinds of images. The principle of Gabor wavelet transform is described as follows. The Gabor function itself constitutes an non-orthogonal basis to describe a relatively localized frequency with a given basis function and its expansion. Because of this reason, the wavelet transform of the Gabor function can be adopted to perform the feature extraction of iris images by using a set of different scales of filters for obtaining the local characteristics of images with different scales. The two dimensional Gabor function is expressed as:

$$g\left(x,y\right)=\left[\frac{1}{2\pi\sigma_x\sigma_y}\right]\exp\left[-\frac{1}{2}\left(\frac{x^2}{\sigma_x^2}+\frac{y^2}{\sigma_y^2}\right)+2\pi jWx\right] \tag{27}$$

$g\left(x,y\right)$ is regarded as the basis function, and then expanded. This process is to carry out the rotation and scale expansion transformation in order to obtain the Gabor wavelet, whose specific expression is shown as:

$$g_{m,n}\left(x,y\right)=a^{-m}G\left(x^{'},y^{'}\right),\quad a>1,\quad m,n\in Z \tag{28}$$

where, $\left(x^{'},y^{'}\right)=a^{-m}\left(x\cos\theta+y\sin\theta,-x\sin\theta+y\cos\theta\right)$, $\theta=n\pi/M$, M represents the number of directions, and a^{-m} represents the scale factor.

A set of Gabor wavelet filters with different directions and scales are obtained by changing the values of M and n . However, these obtained wavelet clusters are orthogonal to each other. If they are used to filter the images, there will have a large number of redundant information. So when using the Gabor wavelet filter for iris feature extraction, the key step is how to design these function parameters. If the parameter design is reasonable, it can let the redundancy of the image information minimum or the ideal.

Suppose U_L is the minimum frequency of filter center, U_H is the maximum frequency of filter center frequency, M is the number of Gabor wavelet filter directions, and S is the scale of Gabor wavelet filter. According to $U_H=\alpha^{s-1}U_L$, the scale parameter can be calculated by:

$$\alpha=\left(\frac{U_H}{U_L}\right)^{\frac{1}{s-1}} \tag{29}$$

Eq. (30) can be obtained by Eq. (27).

$$\begin{aligned}U_H-U_L&=t+2\alpha t+2\alpha^2t+\ldots+2\alpha^{s-2}t+\alpha^{s-1}t\\&=\frac{\alpha+1}{\alpha-1}\left(\alpha^{2s-1}-1\right)t\end{aligned} \tag{30}$$

Since the half width of the standard deviation δ of Gaussian function is $\sigma\sqrt{2\ln 2}$, its corresponding maximum half width of the filter is $\alpha^{s-1}t=\sigma_u\sqrt{2\ln 2}$. This relationship is fed into Eq. (29) and Eq. (30) to obtain:

$$\sigma_u = \frac{(\alpha-1)U_H}{(\alpha+1)\sqrt{2\ln 2}} \tag{31}$$

According to the prior knowledge, the tangent angle of two adjacent ovals is $\varphi = \pi / M$, so obtain:

$$\frac{(u-U_H)^2}{2\ln 2\sigma_u^2} + \frac{v^2}{2\ln 2\sigma_v^2} = 1 \tag{32}$$

Because of $v = \tan\frac{\varphi}{2}u$, obtain:

$$\left(\sigma_v^2 + \tan^2\frac{\varphi}{2}\sigma_u^2\right)u^2 - 2U_H\sigma_v^2 u + U_H^2\sigma_v^2 - 2\ln 2\sigma_u^2\sigma_v^2 = 0 \tag{33}$$

In the above equation for u , the condition that it can have a real number solution is described as:

$$\sigma_v = \tan\frac{\varphi}{2}\sqrt{\frac{U_H^2}{2\ln 2} - \sigma_u^2} \tag{34}$$

By utilizing Eq. (33) and (34), obtain:

$$\sigma_v = \tan\left(\frac{\pi}{2M}\right)\left[U_H - 2\ln 2\left(\frac{\sigma_u^2}{U_H}\right) - 2\ln 2\left(\frac{\sigma_v^2}{U_H}\right)\right] \left[2\ln 2 - \frac{(2\ln 2)^2\sigma_H^2}{U_H^2}\right]^{-\frac{1}{2}} \tag{35}$$

After a series of theory derivation, the relationship among the parameters of the Gabor wavelet filter is obvious. By determining these five parameters (ω, S , M , U_H and U_L), the other parameters can be easy to be found out. The extracted iris is converted into the polar coordinates so that the Gabor filter has symmetry. The filter with direction $[0,\pi]$ can completely describe the iris information in $[0,2\pi]$ direction. Therefore, the adopted Gabor wavelet filter has five different frequencies (1， $1/2\sqrt{2}$ ， $1/2$ ， $1/2\sqrt{2}$ ， $1/4$) and four different directions ($\pi/4$ ， $\pi/2$ ， $3\pi/4$ ， π). Twenty Gabor wavelet filters are used to normalize the iris images. The results of the normalization are shown in Fig. 15 to Fig. 17.

C. Two-dimensional Discrete Cosine Transform (2D DCT)

The two-dimensional discrete cosine transform is defined as:

$$\mathrm{F}(0,0) = \frac{1}{N}\sum_{x=0}^{N-1}\sum_{y=0}^{N-1} f(x,y) \tag{36}$$

$$\mathrm{F}(0,v) = \frac{\sqrt{2}}{N}\sum_{x=0}^{N-1}\sum_{y=0}^{N-1} f(x,y)\cdot\cos\frac{(2x+1)v\pi}{2N} \tag{37}$$

$$\mathrm{F}(u,0) = \frac{\sqrt{2}}{N}\sum_{x=0}^{N-1}\sum_{y=0}^{N-1} f(x,y)\cdot\cos\frac{(2y+1)u\pi}{2N} \tag{38}$$

$$\mathrm{F}(\mathrm{u,v}) = \frac{\sqrt{2}}{N}\sum_{x=0}^{N-1}\sum_{y=0}^{N-1} f(x,y)\cdot\cos\frac{(2y+1)u\pi}{2N}\cdot\cos\frac{(2x+1)v\pi}{2N} \tag{39}$$

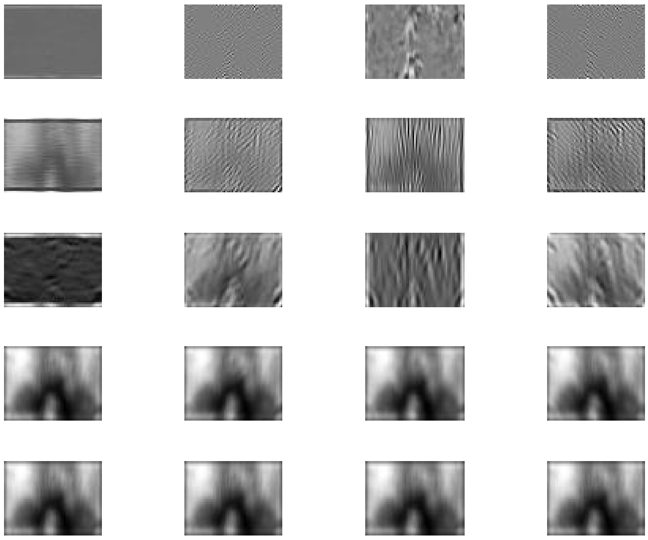

Fig. 15 Real part of iris feature.

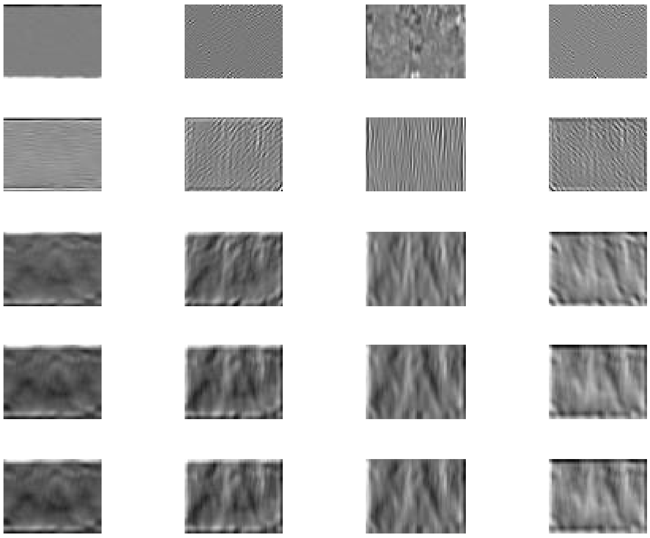

Fig. 16 Imaginary part of iris.

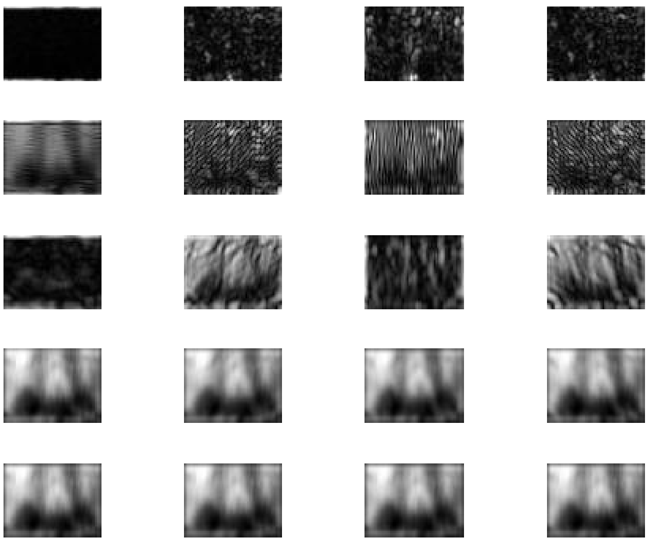

Fig. 17 Combination of real part and imaginary part.

where, $f(x,y)$ is the image space matrix, (x,y) is the position of the current image pixel, and $\mathrm{F}(u,v)$ ($u,v=1,2,\cdots,N-1$) is the transform coefficient matrix.

The two-dimensional discrete transformation is to carry out one-dimensional discrete transformation twice. Fig. 18 is the effect of DCT transformation. According to above results, it can be found that the power of the transformed DCT coefficients is mainly concentrated in the upper left corner, and most of the remaining coefficients are close to zero. It shows that DCT has the characteristics of image compression. Thresholding the transformed DCT coefficient and zeroing the coefficient smaller than a certain value are named as the quantization process in the image compression.The inverse DCT operation is performed to obtain a compressed image. By the same token, if the Gabor filtered image is processed with 2D DCT, its effect is shown in Fig. 19.

(a) Original image

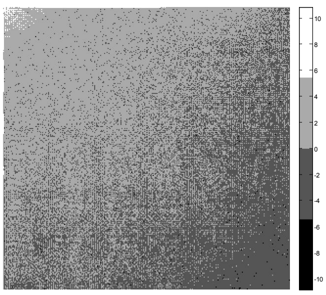

(b) Transferred image

Fig. 18 DCT transform effect.

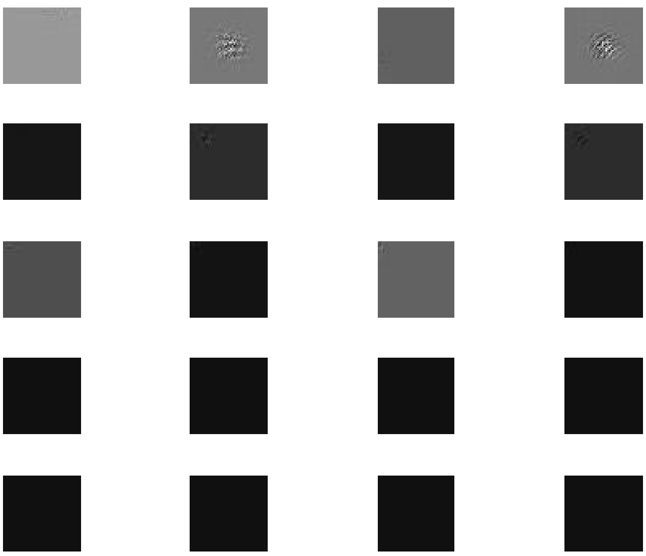

Fig. 19 DCT processing after filtering.

Most of the energy of the image after 2D DCT processing is concentrated in the DC part, that is to say the energy is concentrated in the upper left corner of Fig. 19, which can remove the correlation between the images and make the image coding simple. For the image feature extraction, a small amount of information in the upper left corner can be extracted as the effective information of the image, which can greatly compress the image. Thus this is the principle of dimension reduction of DCT.

D. Iris Recognition Based on Improved Gabor Wavelet

According to the principle of Gabor wavelet, the Gabor filter processes all pixels in the entire image, which will make Gabor filter recognition rate relatively higher. However, not all pixels are the feature points of the image, that is to say the feature point of the image is only a small part of the image pixels. Therefore, the Gabor filter does a great deal of useless work so as to result in a great increase of recognition time. When using the Gabor filter, it must be considered how to reduce the recognition time.

After image processing by the 2D DCT, the image is mainly focused on DC parts. If considering to use 2D DCT to process the image firstly, and only capturing the image in the the upper left corner, a large number of useless information can be removed and the main message is left, which greatly reduces the workload of the Gabor filter. On the other hand, the Gabor filter is slow and laborious, and the 2D DCT can greatly reduces the recognition time. 2D DCT can remove the correlation among images to a certain extent, which is helpful to improve the recognition rate.

In this paper, the idea of this improved Gabor wavelet filter is to process the image first through 2D DCT, and intercept a small portion of the upper left corner, compress the image effectively, then extract the features by Gabor wavelet. Thereby the recognition time will be greatly improved and the recognition rate will also be improved to some extent.

V. Iris Recognition Classification

A. Minimum Distance Classifier

The minimum distance classifier is one of the most commonly used distance classifiers. Firstly, the class centers of known samples (class average) are calculated. Then the samples to be identified are classified as the class where the nearest class center is located.

In an n -dimensional space, A is defined as the name of the category, X_A is the feature set of samples, x_{An} is the characteristic set of the n -th dimensions of class A, μ_A is the mean of A, and μ_{An} is the mean of the n -th feature set. The minimum distance taxonomy first calculates the mean of all dimension of each known class $X_A=(x_{A1},x_{A2},x_{A3},\ldots x_{An})$, which will form an average vector $\mu_A=(\mu_{A1},\mu_{A2},\mu_{A3}\ldots\mu_{An})$. In the same way, the mean vector $\mu_B=(\mu_{B1},\mu_{B2},\mu_{B3}\ldots\mu_{Bn})$ of another category $X_B=(x_{B1},x_{B2},x_{B3}\ldots x_{Bn})$ is calculated. Then the distances from X to X_A and X_B are calculated respectively to obtain $d(x,\mu_A)$ and $d(x,\mu_B)$.

B. Classifier Distance

After the iris samples undergo the feature extraction process, the feature space formed by these feature vectors is finally formed. Therefore, how to calculate the similarity between the samples can be achieved by calculating distance or angle. Given the vectors x and y, the common similarity measures include the following four distances. In this paper, the Euclidean distance is selected as the classifier distance.

1. Euclidean distance

$$d(x,y)=\|x-y\|=\sqrt{\sum_{i=1}^{n}(x_i-y_i)^2} \tag{40}$$

2. Block Distance

$$d(x,y)\sum_{i=1}^{n}|x_i-y_i| \tag{41}$$

3. Mahalanobis distance

$$d(x,y)=(x-y)^T C^{-1}(x-y) \tag{42}$$

where, C is the covariance matrix of the model, which can be simplified as:

$$d(x,y)=\sum_{i=1}^{n}\frac{x_i y_i}{\sqrt{\lambda_i}} \tag{43}$$

where, λ_i is the variance of the i-th component.

4. Cosine angle

$$d(x,y)=\frac{x\cdot y}{\|x\|\|y\|}=\frac{\sum_{i=1}^{n}x_i y_i}{\sqrt{\sum_{i=1}^{n}x_i^2}\sqrt{\sum_{i=1}^{n}y_i^2}} \tag{44}$$

VI. Simulation Experiments and Results Analysis

Simulation experimental environment is described as follows. Windows 10-64 bit operating system, the memory is 8G, the processor is Intel (R) Core i7 7th Gen, MATLAB R2014a simulation software. Five iris images are randomly selected as test images, and their number are set as 1-5. On the same time, each test picture has two corresponding iris pictures as training images, so there is a total of 10 training images. The differences of iris recognition time and iris recognition rate are compared between the improved Gabor wavelet transform method and the unimproved method. Fig. 20 shows the Iris images in Casia iris database. The recognition results are show in Fig. 21 and Fig. 22. It can be seen from the above simulation results that the recognition time based on the improved Gabor wavelet transform is significantly faster than the recognition time without improved method. The recognition time has improved at least 4s. The simulation results fully shows the validity of the improved algorithm.

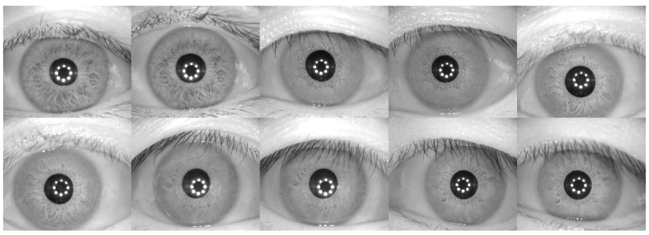

Fig. 20 CASIA iris database.

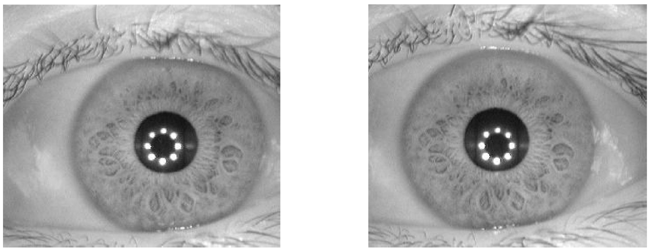

(a) Test image (b) Equivalent image

Fig. 21 Recognition results.

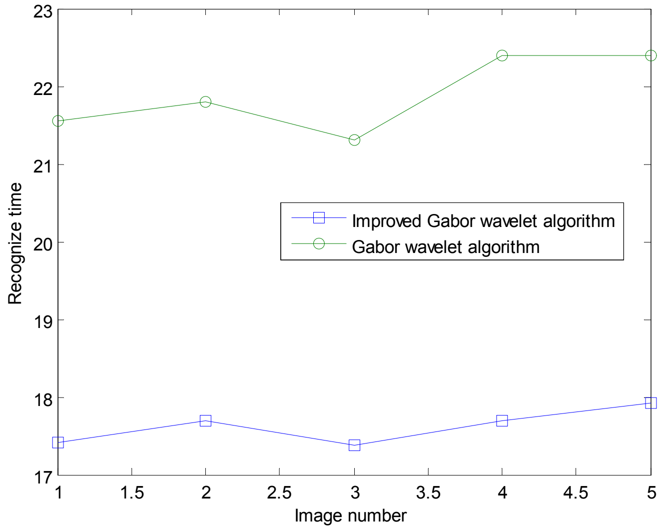

Fig. 22 Comparison of recognition time.

VII. Conclusions

The processing of the human eye images includes the iris localization, iris extraction and iris normalization, etc. In this paper, two classical iris processing processes (Hough transform and edge detection two-step method to locate the iris and calculus operator localization iris) are described in detail. In this process, an improved two-step positioning inner circle is proposed by using the regional growth method. In the iris feature extraction process, the improved Gabor wavelet transform is adopted to extract the iris feature, which is one of the highlights of this article. The Gabor wavelet transform is compared with non improved algorithms, and the simulation results show the effectiveness of the improved algorithm. Finally, the recognition experiments were successfully carried out, and the improved algorithm has greatly reduced the recognition time.

References

[1] A. Gholipour, O. Afacan, I. Aganj, B. Scherrer, S. P. Prabhu, and M. Sahin, et al, "Super-resolution reconstruction in frequency, image, and wavelet domains to reduce through-plane partial voluming in MRI," *Medical Physics*, vol. 42, no. 12, pp. 6919-6932, 2015.

[2] K. Y. Shin, Y. G. Kim, and K. R. Park, "Enhanced iris recognition method based on multi-unit iris images," *Optical Engineering*, vol. 52, no. 4, pp. 047201, 2013.

[3] X. Liu, and Y. J. Jiang, "Fingerprint spoof detection using gradient co-occurrence matrix," *Engineering Letters*, vol. 25, no. 4, pp. 360-365, 2017.

[4] E. P. Kang, "Fuzzy difference-of-Gaussian-based iris recognition method for noisy iris images," *Optical Engineering*, vol. 49, no. 6, pp. 128-140, 2010.

[5] K. K. Mei, A. Cangellaris, and D. J. Angelakos, "Conformal time domain finite difference method," *Radio Science*, vol. 19, no. 5, pp. 1145-1147, 2016.

[6] R. M. Spitaleri, and L. Corinaldesi, “A multigrid semi - implicit finite difference method for the two - dimensional shallow water equations,” *International Journal for Numerical Methods in Fluids*, vol. 25, no. 11, pp. 1229-1240, 2015.
[7] G. Cao, B. Wang, Haro-Carrión Xavier, D. Yang, and J. Southworth, “A new difference image creation method based on deep neural networks for change detection in remote-sensing images,” *International Journal of Remote Sensing*, vol. 38, no. 23, pp. 7161-7175, 2017.
[8] G. J. Hou, G. D. Wang, Z. K. Pan, B. X. Huang, H. Yang, and T. Yu, “Image enhancement and restoration: state of the art of variational retinex models,” *IAENG International Journal of Computer Science*, vol. 44, no.4, pp. 445-455, 2017.
[9] J. Petrovich, and M. Reimherr, “Asymptotic properties of principal component projections with repeated eigenvalues,” *Statistics & Probability Letters*, no. 130, pp. 42-48, 2017.
[10] P. Yang, J. Gao, and W. Chen, “Curvelet-based POCS interpolation of nonuniformly sampled seismic records,” *Journal of Applied Geophysics*, vol. 79, no. 79, pp. 90-99, 2012.
[11] Y. Liu, and L. Dong, “Iterative reduction of out-of-band power and peak-to-average power ratio for non-contiguous OFDM systems based on POCS,” *Ieice Transactions on Communications*, vol. 100, no. 8, pp. 1489-1497, 2017.
[12] C. Li, W. Zhou, and S. Yuan, “Iris recognition based on a novel variation of local binary pattern,” *Visual Computer*, vol. 31, no. 10, pp. 1419-1429, 2015.
[13] S. Umer, B. C. Dhara, and B. Chanda, “Iris recognition using multiscale morphologic features,” *Pattern Recognition Letters*, vol. 65, no. C, pp. 67-74, 2015.
[14] M. D. Marsico, A. Petrosino, and S. Ricciardi, “Iris recognition through machine learning techniques: a survey,” *Pattern Recognition Letters*, no. 82, pp. 106-115, 2016.
[15] S. H. Hsieh, Y. H. Li, C. H. Tien, and C. C. Chang, “Extending the capture volume of an iris recognition system using wavefront coding and super-resolution,” *IEEE Transactions on Cybernetics*, vol. 46, no. 12, pp. 3342-3350, 2016.
[16] N. Zhou, H. Tian, G. Li, P. Dong, and L. Qing, “Quantum image encryption based on generalized Arnold transform and double random-phase encoding,” *Quantum Information Processing*, vol. 14, no. 4, pp. 1193-1213, 2015. 2015, 14(4):1193-1213.
[17] Z. Liu, C. Shen, J. Tan, and S. Liu, “A recovery method of double random phase encoding system with a parallel phase retrieval,” *IEEE Photonics Journal*, vol. 8, no. 1, pp. 1-7, 2016.
[18] S. Liu, B. M. Hennelly, C. Guo, and J. T. Sheridan, “Robustness of double random phase encoding spread-space spread-spectrum watermarking technique,” *Signal Processing*, vol. 109, no. 43, pp. 345-361, 2015.
[19] L. Yan, L. Fei, C. Chen, Z. Ye, and R. Zhu, “A multi-view dense image matching method for high-resolution aerial imagery based on a graph network,” *Remote Sensing*, vol. 8, no. 10, pp. 799, 2016. 2016, 8(10):799.
[20] D. Li, “A novel method for multi-angle SAR image matching,” *Chinese Journal of Aeronautics*, vol. 28, no. 1, pp. 240-249, 2015.
[21] N. Note, P. De Smedt, T. Saey, W. Gheyle, B. Stichelbaut, and V. D. B. Hanne, et al, “Removal of sensor tilt noise in fluxgate gradiometer survey data by applying one - dimensional wavelet filtering,” *Archaeological Prospection*, no.4, pp. 1-8, 2017.
[22] N. Onizawa, D. Katagiri, K. Matsumiya, W. J. Gross, and T. Hanyu,” Gabor filter based on stochastic computation,” *IEEE Signal Processing Letters*, vol. 22, no. 9, pp. 1224-1228, 2015.
[23] L. Zunino, and H. V. Ribeiro, “Discriminating image textures with the multiscale two-dimensional complexity-entropy causality plane,” *Chaos Solitons & Fractals*, no. 91, pp. 679-688, 2016.
[24] J. Ko, A. J. Kurdila, J. L. Gilarranz, and O. K. Rediniotis, “Particle image velocimetry via wavelet analysis,” *Aiaa Journal*, vol. 36, no. 8, pp. 1451-1459, 2015.
[25] A. S. Kozlova, “Method of digital hologram coding–decoding and holographic image processing based on the Gabor wavelet,” *Russian Physics Journal*, vol. 58, no. 10, pp. 1475-1476, 2016.
[26] A. Czajka, and K. W. Bowyer, “Presentation attack detection for iris recognition: an assessment of the state of the art,” *ACM Computing Surveys*, vol. 51, no. 4, pp. 1-35, 2018.

Xiao-Hong Chen received her B. Sc. And M. Sc. degrees in control science from University of Science and Technology Liaoning, China in 1999 and 2002, respectively. She is currently a lecturer in School of Mechanical Engineering and Automation, University of Science and Technology Liaoning. Her main research interest is image processing and pattern recognition.

Jie-sheng Wang received his B. Sc. And M. Sc. degrees in control science from University of Science and Technology Liaoning, China in 1999 and 2002, respectively, and his Ph. D. degree in control science from Dalian University of Technology, China in 2006. He is currently a professor and Master's Supervisor in School of Electronic and Information Engineering, University of Science and Technology Liaoning. His main research interest is modeling of complex industry process, intelligent control and Computer integrated manufacturing.

Yan-lang Ruan is currently a master student in School of Electronic and Information Engineering, University of Science and Technology Liaoning, China. His main research interest is image processing and pattern recognition.

Shu-Zhi Gao received the B. Sc. degree from Shenyang University of Chemical Technology, China in 1989, and received the M. Sc. degrees from Northeastern University, China in 2012. She is currently a professor and Ph. D. supervisor in Shenyang University of Chemical Technology. Her research interests include feedback control system, modeling of complex industry process and intelligent control.